

Soft-Phonon-Induced Raman Scattering in IV-VI Compounds

T. Shimada, K. L. I. Kobayashi, Y. Katayama, and K. F. Komatsubara

Central Research Laboratory Hitachi, Ltd., Kokubunji, Tokyo 185, Japan

(Received 31 August 1976; revised manuscript received 6 May 1977)

At both the cubic-rhombohedral phase-transition temperature T_c and the zero-gap temperature T_b , anomalous increases in Raman intensities are observed in $\text{Pb}_{1-x}\text{Sn}_x\text{Te}$ (for $x=0-1$) single crystals. These are attributed to Raman scattering enhanced by the softening of the TO phonon near T_c and also allowed by enhanced interband-mixing effects near T_b . These interband-mixing effects not only enhance the Raman intensity, but also increase T_c .

We have observed anomalous increases in Raman intensities in $\text{Pb}_{1-x}\text{Sn}_x\text{Te}$ single crystals with various composition $x=0-1$ at both the cubic-rhombohedral phase-transition temperature T_c and the band-inversion temperature T_b , where the band gap becomes just zero. These anomalous increases are attributed to Raman scattering, which is forbidden in the high-temperature phase of NaCl-type structures, induced mainly by the fluctuation of the order parameter enhanced by the softening of the TO phonons near T_c and also induced by enhanced interband-mixing effects near the zero-gap temperature T_b .

The displacive phase transition in narrow-gap semiconductors such as PbTe and SnTe at low temperatures is an interesting phenomenon in which interband-mixing effects may play an important role.¹ In this Letter, in order to investigate the effects of interband mixing on the phase transition, Raman spectra and their temperature dependences have been systematically studied in the $\text{Pb}_{1-x}\text{Sn}_x\text{Te}$ pseudobinary alloy whose band gap varies with x .

The Raman scattering spectra were taken with a Cary-82 Raman spectrometer using a CR-50 Kr-ion laser. The measurements were made in a backscattering geometry for {100} or {110} surfaces of $\text{Pb}_{1-x}\text{Sn}_x\text{Te}$ single crystals ($x=0, 0.24, 0.39, 0.43, 0.54, \text{ and } 1.0$) at temperatures of 10–300 K using a Cryo-Tip variable-temperature Dewar. The crystals were grown by a solution growth or Bridgman methods. Wafers of SnTe were mechanically polished, chemically etched for a few minutes with a solution consisting of six parts by volume CH_3COOH , three parts 70% HNO_3 , and one part 50% HF, and finally rinsed with methanol.² Chemical etchant for $\text{Pb}_{1-x}\text{Sn}_x\text{Te}$ ($x \leq 0.95$) was a solution of one part HBr with Br_2 , and one part methanol. Chemical etching is one of the most important processes for preparing the excellent surface from which the stable and

intense Raman signal comes. The chemical etching and rinse with methanol were made just before setting the sample in the Dewar.

An example of Stokes-Raman spectra from SnTe at 10 K is shown in the inset of Fig. 1. The Stokes-Raman spectrum consists of two peaks at 131 and 147 cm^{-1} . The intensity of the 131- cm^{-1} band is about twice that of the 147- cm^{-1} band, and the widths of both bands are about 7 cm^{-1} . Brillson, Burstein, and Muldrew² have previously reported a peak at around 132 cm^{-1} with a width of 21 cm^{-1} . This might be the envelope of our two peaks. The stronger peak at 131 cm^{-1} is assigned as the Raman peak of unscreened LO phonons near the Γ point,² while the weaker peak at 147 cm^{-1} is tentatively assigned as overtones of TO phonons near the X points where the state density

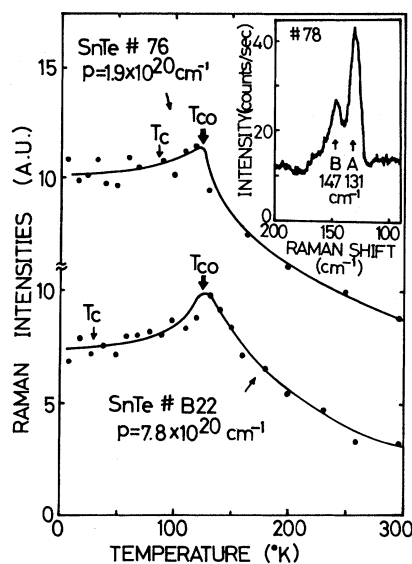


FIG. 1. Temperature dependence of Raman intensity of the 131- cm^{-1} peak in two SnTe crystals with different carrier concentrations. Inset: Stokes-Raman spectra from SnTe at 10 K.

of phonons is maximum.³

Peak positions and bandwidths vary very slightly as functions of temperature. The Raman intensity of the 131-cm^{-1} peak for two SnTe crystals with different carrier concentration is shown as a function of temperature in Fig. 1. The bulk phase-transition temperature T_c strongly depends on carrier concentration.⁴ As seen in Fig. 1, the temperatures at which the Raman intensity becomes maximum are the same in two SnTe crystals, and coincide with the phase-transition temperature T_{c0} for zero carrier concentration.⁴ The penetration depth of the incident laser light is estimated to be about 100 \AA and it is of the same order as the thickness of the depletion layer in PbSnTe samples with carrier concentrations of $10^{19}\text{--}10^{20}\text{ cm}^{-3}$ and with large dielectric constants of $10^3\text{--}10^4$. These facts suggest that the Raman signals come from the surface depletion layer.

Because SnTe has the NaCl structure above T_c , first-order Raman scattering is forbidden at temperatures above T_c . The Raman intensity should increase with decreasing temperature below T_c , as schematically shown in Fig. 2, curve *a*. In contrast to this expectation, Raman scattering was actually observed above T_c . Moreover, it was enhanced anomalously near T_c .

We now consider the possible reasons for these anomalous behaviors. First, the surface electric-field-induced Raman-scattering mechanism⁵ should be examined because the Raman signal comes from the surface depletion layer. We consider this effect as due to the atomic-displacement mechanism because the TO-mode frequency is low and the field-induced displacement becomes relatively large. Curve *b* in Fig. 2 shows the qualitative temperature dependence of the Raman intensity which is a result of self-consistent calculation of polarization and displacement induced by the surface field taking into account the effects of TO-phonon softening. Within this model, an anomalous kink at the T_c is expected. However, the peaking of Raman intensity is not explained in this model.

Second, we consider the soft-phonon-induced mechanisms. Since the peak position and the

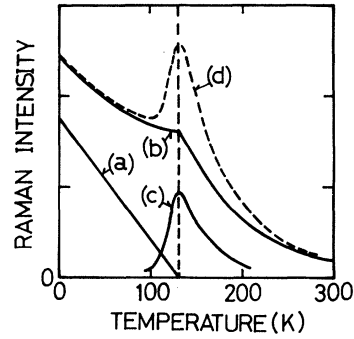


FIG. 2. Schematic temperature dependences of Raman intensity caused by static displacement by the phase transition (curve *a*), surface-field-induced displacement (curve *b*), fluctuation-induced displacement enhanced by softening of TO phonons (curve *c*), and combined surface-field and fluctuation effects (curve *d*).

bandwidth of the observed Raman spectrum, which should vary depending upon temperature especially near T_c when the two-phonon mechanism dominates, change very little in the wide range of temperature, the observed Raman peak cannot be attributed to two-phonon scattering mechanisms involving both LO and TO phonons. Therefore, as a simplest case of the soft-phonon-induced Raman scattering mechanisms, we conjecture that softening of TO modes will allow first-order Raman scattering by LO phonons through enhancement of fluctuations of the order parameter near T_c . To treat this model rigorously, one would have to obtain the vibronic state of the electron-soft-TO-phonon system. For simplicity, however, we take the effect of soft TO phonons into account as the mixing of valence-band (*V*) and conduction-band (*C*) characters. Within the two-band approximation, the valence-band wave function $|V'\rangle$ is expressed as⁴

$$|V'\rangle = |V\rangle + \sum \frac{\langle V|\mathcal{H}_{TO}|C\rangle}{E_C - E_V} |C\rangle + \dots \quad (1)$$

Using the approximate wave function (1), the Raman-scattering probability R_{LO} , which is proportional to the square of the electron-LO-phonon matrix element M , is obtained as

$$R_{LO} \propto |M|^2 = |\langle V'|\mathcal{H}_{LO}|V'\rangle|^2 = \left| \langle V|\mathcal{H}_{LO}|V\rangle + \langle V|\mathcal{H}_{LO}|C\rangle \sum \frac{\langle V|\mathcal{H}_{TO}|C\rangle}{E_C - E_V} \right|^2 + \dots \quad (2)$$

The first term vanishes in the NaCl structure as described previously. The second term can be eval-

uated within the deformation-potential approximation.⁴ Then, R_{LO} is expressed as

$$R_{LO} \propto \begin{cases} \frac{T}{(E_c - E_v)^2 (T - T_c)} | \langle V | \mathcal{H}_{LO} | C \rangle |^2, & \text{for } T > T_c, \\ \frac{T}{2(E_c - E_v)^2 (T_c - T)} | \langle V | \mathcal{H}_{LO} | C \rangle |^2, & \text{for } T < T_c, \end{cases} \quad (3)$$

where $\omega_{TO}^2 = C(T - T_c)$. This relation explains the enhancement of the Raman intensity at the temperature $T - T_c$ as schematically shown by the curve c in Fig. 2. Furthermore, this relation predicts that the Raman intensity should be enhanced at $T = T_b$, where the band gap E_c becomes zero.

In order to elucidate this enhancement near T_b , the temperature dependence of the Raman spectrum was measured for $Pb_{1-x}Sn_xTe$ with various compositions. As is seen in Fig. 3, the Raman intensities are enhanced anomalously at temperatures $T = T_b$ as well as $T = T_c$.

In Fig. 4 the phase-transition temperature T_c (dotted open circles) and the band-inversion temperature T_b (open circles) obtained in this study are shown together with the values obtained by other methods.^{4,6-11} The small filled circles, which were determined from capacitance experiments with p - n junctions,¹¹ should correspond to the phase-transition temperature for zero carrier concentration T_{c0} . As mentioned before, the T_{c0}

determined by the present Raman experiment is equal to the T_{c0} in SnTe. As seen in Fig. 4, the T_c 's obtained in this study and the T_{c0} 's mentioned above fall naturally along the same curve when plotted versus the composition x . This means that the phase-transition temperature T_c 's obtained here by Raman experiment correspond to the T_{c0} 's for zero carrier concentration and thus the carriers in PbSnTe are depleted at surface.

T_{c0} increases with increasing x showing a temperature kink at around $x = 0.47$ where T_{c0} coincides exactly with T_b . This suggests that the decrease in band gap E_c raises the phase-transition temperature remarkably. This postulate may be discussed in terms of the same soft-TO-phonon-electron interaction mentioned above. The TO-phonon frequency renormalized with the TO-pho-

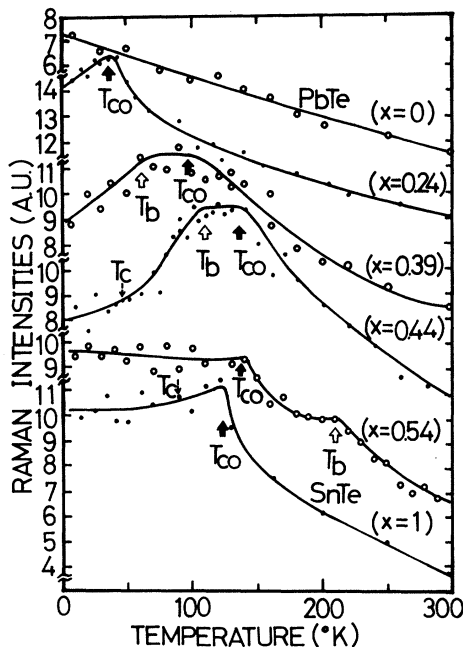


FIG. 3. Temperature dependence of Raman intensity of the 131-cm^{-1} peak in $Pb_{1-x}Sn_xTe$ on composition x .

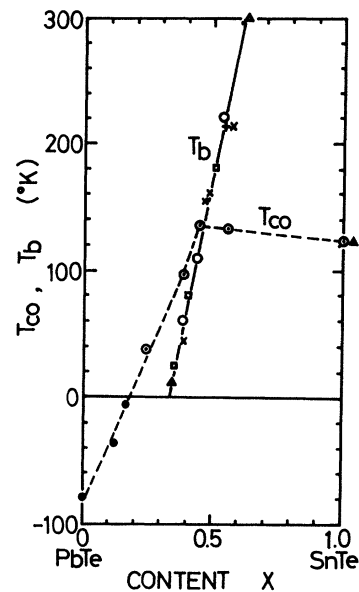


FIG. 4. Phase-transition temperatures T_{c0} for zero carrier concentration and band-inversion temperatures are shown as functions of composition x for $Pb_{1-x}Sn_xTe$. Data points T_b 's (\circ) and T_{c0} 's (\odot) were determined in this work. The T_b 's [\square (Ref. 4), Δ (Ref. 5), \times (Ref. 6), and $+$ (Ref. 7)] and the T_{c0} 's [\bullet (Ref. 8) and Δ (Ref. 2)] were obtained by other investigators.

non-electron interaction $\hat{\omega}_{\text{TO}}$ is expressed as⁴

$$\hat{\omega}_{\text{TO}}^2 = \omega_{\text{TO}}^2 - \frac{4g}{(2\pi)^3} \int_w^0 \left(\frac{\hbar D^2}{2MNa^2} \right) \frac{\rho(E)dE}{E_G + 2E}, \quad (4)$$

where w is the bandwidth. This equation indicates that the $\hat{\omega}_{\text{TO}}^2$ can most easily become negative near $E_G = 0$. This means that T_{c0} peaks at around $x = 0.47$ and coincides exactly with T_b .

In summary, an anomalous increase in Raman intensity due to unscreened LO phonons was observed at both temperatures T_c and T_b which correspond to the displacive phase transition and the band inversion, respectively. It is shown that the electron-soft-TO-phonon interaction plays an important role in the displacive phase transition in PbSnTe.

We wish to acknowledge fruitful discussions with Professor H. Kawamura of Osaka University and also wish to thank Y. Kato for stimulating discussions and sample preparation, and J. Umeda for his encouragement during this work.

¹N. Kristoffel and P. Konsin, *Phys. Status Solidi* **21**,

K39 (1967).

²L. J. Brillson, E. Burstein, and L. Muldower, *Phys. Rev. B* **9**, 1547 (1974).

³E. R. Cowley, J. K. Darby, and G. S. Powley, *J. Phys. C* **2**, 1916 (1969).

⁴K. L. I. Kobayashi, Y. Kato, Y. Katayama, and K. F. Komatsubara, *Phys. Rev. Lett.* **37**, 772 (1976), and *Solid State Commun.* **17**, 875 (1975).

⁵L. Brillson and E. Burstein, *Phys. Rev. Lett.* **27**, 808 (1971).

⁶G. S. Powley, W. Cochran, R. A. Cowley, and G. Doling, *Phys. Rev. Lett.* **17**, 753 (1966).

⁷C. R. Hews, M. S. Adler, and S. D. Senturia, *Phys. Rev. B* **7**, 5195 (1973).

⁸J. O. Dimmock, I. Melngailis, and A. J. Strauss, *Phys. Rev. Lett.* **16**, 1193 (1966).

⁹J. R. Dixon and R. F. Bis, *Phys. Rev.* **176**, 942 (1968).

¹⁰G. W. Pratt, Jr., and A. Das, *J. Phys. Chem. Solids*, Suppl. **32**, 279 (1971).

¹¹R. T. Bate, D. L. Carter, and J. S. Wrobel, in *Proceedings of the Tenth International Conference on the Physics of Semiconductors, Cambridge, Massachusetts, 1970*, edited by S. P. Keller, J. C. Hensel, and F. Stern, CONF-700801 (U. S. Atomic Energy Commission, Division of Technical Information, Springfield, Va., 1970), p. 125.

Structural Phase Transition in Epitaxial Solid Krypton Monolayers on Graphite^(a)

M. D. Chinn and S. C. Fain, Jr.^(b)

Department of Physics, University of Washington, Seattle, Washington 98195

(Received 8 April 1977)

Lattice-constant measurements of epitaxial solid krypton monolayers adsorbed on the basal plane of graphite reveal an apparently second- (or higher-) order structural phase transition from an in-registry $(\sqrt{3} \times \sqrt{3})30^\circ$ structure to an out-of-registry compressed structure. Measurements as a function of equilibrium vapor pressure were made with a high-resolution, low-energy-electron diffraction apparatus for three temperatures near 57 K. Indirect evidence for spatial modulation of the compressed structure by the substrate potential is presented.

We show here that a solid Kr layer adsorbed on the basal plane of graphite undergoes an apparently second- (or higher-) order phase transition from an in-registry, $(\sqrt{3} \times \sqrt{3})30^\circ$ structure to an out-of-registry, compressed structure as the Kr pressure above the substrate is increased. This transition was first inferred from vapor-pressure isotherms,¹ but was not observed in an earlier low-energy-electron diffraction (LEED) investigation.² We observe this transition with high-resolution LEED³ and report the first detailed measurements of mean overlayer lattice constant as a function of the equilibrium vapor pressure P . Our observations are inconsistent with the first-

order, in-registry to out-of-registry transition recently proposed for Kr on graphite.⁴ However, our results show remarkable agreement with a one-dimensional dislocation model of monolayer epitaxy.⁵ The data provide a unique opportunity to test theories of monolayer epitaxy⁵⁻⁸ in a case where the forces involved are fairly well known.

Kr monolayers were condensed on a cleaved, natural graphite crystal mounted in an ultrahigh-vacuum system.³ The Kr pressure was increased in small increments while monitoring the LEED pattern. Parameters for the normal-incidence electron beam were 144 eV, 3 nA, and 0.2 mm diam. Electrons backscattered within 30° of nor-